Characterizing Excitatory and Inhibitory Neuron Responses to Dark and Bright Stimuli in the Visual Cortex of Awake Mice

Lisa Meyer-Baese

Introduction

A long-standing and fundamental goal of neuroscience revolves around understanding the neural basis of visual perception. Recently the use of mice to better model mechanics of visual circuits has become a larger focus (Huberman et al., 2011). The motivation behind this method is that mice are unrivaled in terms of the variety of technological tools that exist to monitor and label specific cell types and circuits.

To understand the neural basis for visual perception, electrical probes must be placed in the primary visual cortex, V1. Neuronal activity in the brain gives rise to transmembrane currents, which are measured using micro-machined silicon electrode arrays (Buzsáki,2004). These electrodes are used to measure large numbers of neurons and monitor local neural circuits during sensory stimulation. One quantifiable measurement is the action potential of neurons (spikes), occurring when the membrane potential of a cell rapidly rises and falls. When the neuron's action potential crosses a certain threshold, it is said to fire and transmit information to other downstream neurons. Another quantifiable metric is the local field potential (LFP). These are transient electrical signals generated by the summed electrical activity of individual neurons.

This area is divided in 6 horizontal layers, each having characteristic distribution of inputs and outputs across layers. Feed-forward inputs from the lateral geniculate nucleus of the thalamus (LGN) arrive in layer 4 and depart to other cortical areas from layer 2/3 (Douglas et al., 1998). Electrode probes transverse and record from layers 2 through 6 corresponding to 200-1200 microns in depth. Neurons in each layer have distinctive receptive-field properties. Neurons on the superficial layers have small receptive fields whereas deeper neurons have larger ones (Kandel, et al., 2005).

There are two major types of signals in the visual system, the ON and OFF pathways, that are used for the detection of luminance increments and decrements (Komban et al., 2011) Several studies have shown that these two pathways are not mirror images of each other, but rather that their responses are asymmetric (Pandarinath et al., 2010). It is because of this asymmetry that humans can read black text on white paper faster than white text on black paper (Buchner et al., 2007).

Neurons within these layers of V1 can be assigned to one of two classes: inhibitory or excitatory. These neurons can be distinguished based on the action potential wave form they produce. One type of inhibitory neuron, termed fast spiking neurons, have a narrow peak-to-trough width. Broader action potential waveforms typically arise from excitatory neurons. The way these two classes of neurons in the mouse V1 respond to bright and dark visual stimuli can be recorded using the aforementioned probes.

The goal of this study is to characterize how excitatory and inhibitory neurons in the mouse V1 respond to dark and light visual stimuli, in both time and space. To do this, the mice will be shown a visual stimulus at different positions on the screen throughout the duration of an experiment (Fig 1). The stimulus shown is a vertical bar which is 50 degree high by 9 degrees wide, ranging in color from black (0) to white (255). The intensity of a pixel is expressed within a given range between a minimum and a maximum. This range is represented in an abstract way as a range from 0, total absence, all the way to 255 total presence (Speed et al., 2019). All stimuli are shown against a background whose color corresponds to the mean of this range, at 128. The relationship between the luminance of a brighter area of interest and that of an adjacent darker area is called luminance contrast. Michelson Contrast measures the relation between the spread and the sum of two luminances which is what is what is used in this experiment, rather than the pixel values (Wiebel et al., 2016). The mouse’s real time neural response to all stimuli gets recorded by the inserted probe over the duration of the experiment. This data will then be fed through a spike sorting algorithm that uses the characteristics of individual spike waveforms present in the neural data to distinguish the activity of one or more neurons from background neural activity.

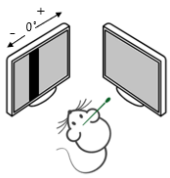

Figure 1 Experimental Set-Up

The output for each experiment will be the firing times for the different neurons within the visual cortex. Given the firing times of the neurons, as well as the stimulus times, one can now begin to quantify the encoding in mouse V1 of bright versus dark stimuli. To do this different methods of data processing and computational modeling will be applied to gain further insight on the cooperative behavior of neurons which in turn increases our understanding of how these processes impact our visual perception.

An increased understanding in mouse V1 will allow us to better characterize the internal electrical and neural circuit mechanisms of the visual process. This understanding is a necessary step towards technologies of the future that may, for example, directly generate synthetic visual perception in the brain by a visual prosthesis that stimulates ON and OFF pathways to remedy visual dysfunctions, such as acquired blindness.

Literature Review

Understanding the relationship between structure and function in the brain allows investigators to determine what circuits underlie specific visual computations. One particular region of interest in the brain is the primary visual cortex (V1). The fundamental task carried out by visual neurons is the "encoding" of luminance increments (white on grey) versus decrements (black on grey). To bridge the gap between structure and function two aspects of the cortex are studied: the neurons along with their wiring and the functional computations that get performed by the circuit.

One of the earliest and most significant contributions to this field of research was done by Hubel and Wiesel in 1959. They revealed the fundamental properties of visual coding in the cortex. They discovered that neurons transform the pixels of light hitting the retina into responses that are selective to the orientation of the input stimulus. Six years prior to this, Kuffler showed that ganglion cells in the retina have concentric receptive fields, with an 'on' and 'off' periphery. Hubel and Wiesel figured out that these 'on' and 'off' areas were divided into excitatory and inhibitory areas. These two areas are arranged within a receptive field in a side-by-side fashion, where the central area of one type is bordered by antagonistic areas of the other type. It was also discovered early on that neurons that are vertically aligned in V1 have receptive fields that are also aligned in visual space (Woolsey et al., 1970).

Since then, many more discoveries have been made regarding the intricacies of the visual cortex. Research indicated that the neurons in the visual cortex are not only sensitive to orientation but also color. A recent study (Komban et al., 2011) shows that darks are detected more rapidly and accurately than lights. However, it was demonstrated that there are many more black-dominant than white-dominant responses in layer 2/3 neurons of V1 in macaque monkeys (Xing et al., 2010). The suggestion that the OFF pathway is stronger than the ON pathway was also validated in other studies which also used higher mammals (Yeh et al., 2009; Jansen et al., 2018).

It was noted that the black-over-white preference is generated or at the very least amplified in V1 (Yeh et al., 2009). These results coincided with findings that used EEG and fMRI recording modalities which showed that decrements are stronger than increments in humans. Ten years later this was again validated and further studied by looking into the factors that modulate the OFF dominance (Jansen et al., 2018). This study discovered that the dominance is modulated by the size and spatial frequency of the stimulus. OFF-dominated responses are driven five times more than ON-dominated neurons when the large grating patterns have a low spatial frequency. When this grating size decreases, and when the spatial frequency increases, then this OFF dominance is reduced. This happens as the stimulus is moved further away from the observer. It was concluded that cortical OFF dominance is continuously adjusted by a neuronal mechanism that modulates ON/OFF response balance depending on the input stimuli.

So far most studies directly recording single neurons have been mainly performed in the anesthetized animals. This study is novel in that it aims to extend these findings to the awake visual cortex, and to multiple retinotopic locations in primary visual cortex of mice. This project will establish spatial and temporal constraints for how neural activity must be directly activated in a mouse's V1 to code ON versus OFF responses. To characterize how excitatory and inhibitory neurons in mice V1 respond to bright and dark visual stimuli the mice are presented with input stimulus of different colored bars, ranging in luminance defined by Michelson Contrast. Their response to these stimuli is recorded using multi-shank probes that are placed in the visual cortex of the mice. The aim is to use this data to gain insight on, and to characterize differences between, the different classes of neurons within the different layers of V1. Once neurons are identified as being inhibitory and excitatory, their response properties can then be tied back to the different input stimuli. The objective is to gain a better understanding of how the brain processes and relays visual stimuli to parts of the brain downstream of V1.

Methodology

All data was acquired from prior experiments in the lab. For detailed methods review Speed et. al., 2019.

Implant Surgery:

Custom stainless steel headplates with recording chambers were implanted in male wild type C57Bl6 (RRID: IMSR_JAX:000664) and PV-Cre mice (RRID: IMSR_JAX:017320). This was done under isoflurane anesthesia. The headplate was affixed to the skull using a thin layer of veterinary adhesive called VetBond then securely bonded to the cranium with a dental cement (Metabond). The recording chamber was then sealed with elastomer KwikCast. After the implantation mice were given 3 days to fully recover. Following recovery, the mice were handled and habituated for 3-4 days in the head fixation apparatus.

Barmapping Stimulus:

Vertical bars, 50 degrees high and 9 degrees wide, were presented in 17 locations. These ranged from -40 to 115 degrees in the mouse's visual field, at various contrasts between 0 and 100% for black and white. The stimuli presented is across two monitors as seen in figure 1, where the vertical bars span the entire elevation range and change across azimuth. Bars were displayed 10 times in each location and contrast combination (0.1s duration, 0.3s interval).

Electrophysiology:

Recordings were performed using multi-site NeuroNexus linear probes consisting of one 32- channel shank. Each "channel" represents an electrode pad that captures extracellular voltage, and is referenced to a different, common electrode. Thus, the activity of the brain as represented by electrical potentials generated by neurons, can be captured. Electrodes were advanced ~1000um below the cortical surface to ensure all contacts sampled all layers of cortex. Data was collected for the duration of the recording session which was typically around 2000 trials (dependent on the number of contrasts shown). The craniotomy was kept sterile and covered with silicone elastomer in between consecutive recording days. Data was recorded in the left hemisphere of V1. Each recording was either localized to the monocular or binocular region of V1.

Data Analysis: Spike Sorting

The acquired raw electrical signals were amplified and digitized using Blackrock Microsystems then exported for post processing. Extracellular spikes were isolated using the KlustaViewa Suite. Neuron action potentials, or spikes, are rapid events of change in electrical potential that can be captured and identified in the amplified data. The spike-sorting pipeline involves three main steps: (i) spike detection and feature extraction, (ii) cluster analysis, and (3) manual curation (Rossant et al., 2016). Because spikes are rapid events (1-2ms), neural data is first high-pass filtered (>200 Hz). Then, an automatic detection algorithm is often used as a first pass to identify spikes. Spike identification is often liberal at this stage, because false "spikes" can be removed in a later step. This automatic algorithm typically uses either thresholding or template matching to extract spikes. Thresholding is simply

taking all events that breach a certain voltage threshold, while template matching involves calculating the correlation between possible events and a generic "spike" waveform. This automatic algorithm sorts spike events into clusters based on timing and location (channel) of the spike, representative of individual neurons. Thus, any spikes in the cluster are taken to have come from that neuron. Finally, a user manually curates the clusters using PCA analysis and correlation metrics on all spikes in the cluster as aids. The Klusta algorithm uses thresholding in its first pass algorithm.

Then, fast spiking (FS) and Regular Spiking (RS) units were classified according to spike width (peak to trough). Units with a peak-to-trough width less than 0.57ms were classified as FS, while all broader unites were classified as RS (Speed et al., 2019).

Data Analysis: Data Storage

LFP analysis was performed on a set of 156 recordings from 11 mice. These same recordings are used to analyze the single-unit response. The recording number, mouse number, date, and experiment number were added to a new data frame object that will store all information pertaining to the experiments. The location of their corresponding sorted single-unit (spike-sorted) data was identified and added to a database.

An automated accessing function based on the database was coded. It can access and store all properties that are important for a given recording and the corresponding neurons. This includes all the basic properties relevant to an experiment such as the mouse, the date, the base name, and experiment number. Furthermore, it holds other properties of the experiment such those related to input stimuli (the times, the contrasts, etc.), the filtered data and the optimal receptive field. It also holds information pertinent to individual neurons such as their classification (FS/RS) and their depth (L2/3, L4, or L5/6). Internally pulling and storing all variables in one place greatly simplifies further analysis.

Data Analysis: Generating Bar Maps

Bar maps were created by first obtaining the bar presentation times from the photodiode signal. A photodiode is a device that produces a current which is linear with the input light power. This device picks up the stimulus presentation times in real-time, reflecting what the mouse sees. The times from the photodiode signal are therefore the "true" times to which the bar stimulus times from the computer need to be matched up to. The computer "block" file contains its own stimulus times (which could be off due to a lag between when the computer output versus when it is actually displayed), as well as information regarding contrast of the stimulus. With matched times one can extract bar positions and indexes of bar trials by color. The spike data time locked to these events is then taken in 400ms windows, from 100ms before to 300ms after a stimulus presentation.

Once this step is completed a bar map can be made by picking a stimulus of a specific contrast value (Fig 2). For a given experiment all occurrences of that stimulus contrast can be obtained and then sorted by the position at which they occurred on the screen. Per position and contrast there are 10 repeats which can be averaged together. A final heat map of the stimulus-evoked neuron response can then be plotted of position versus time. This heat map – termed a bar-map - reveals the region of visual space where the neural activity exhibits maximum sensitivity. Each row of a bar map, when plotted in 2-D, represents the peristimulus time histogram (PSTH) which is a histogram of binned spike counts versus time. The colors on the heat map represents the count aggregation of this extra dimension. The z-axis for spike plots is therefore the firing rate of the neuron in Hz.

The response of all neurons in a recording can be averaged together to create an average bar-map. The location in space of the lightest and darkest spot, correspond to the activation and suppression of that neuron, which occurs at the optimal receptive field for that neuron. This functionality was incorporated into the automated code across all 156 recordings, accounting for variability.

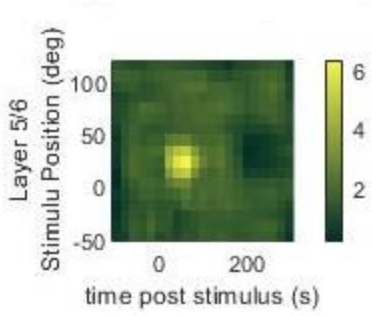

Figure 2 Example population Bar-Map of layer 5/6 response with receptive field at 40 degrees. Yellow spot indicates activation response to stimulus and the dark green is the suppression. The color bar represents the binned spike counts in spikes per second (Hz).

Data Analysis: Determining LFP Matches

Neurons that contribute to a response should have the same or similar optimal receptive field as the LFP data, because LFP is an aggregate signal it is more stable than individual neurons. The Spike data on the other hand is a collection of assorted neurons not all of which are necessarily contributing to the response. To ensure that only relevant neurons are analyzed the average spike response of neurons per layer was compared to that of the LFP data. By hand, each layer was compared and marked as being a match versus mismatch (Fig 2). All results reflect data from only the layers that were matched. It was assumed that if layers matched, then on average the neurons contributing to the layer also matched the LFP receptive field.

Data Analysis: Maximum PSTH

For each recording per neuron the maximum firing rate was determined. The data corresponding to the first 100ms before stimulus onset was averaged and subtracted from all points. This baseline was removed to ensure that the maximum PSTH is that which corresponds to the firing rates as changes from the baseline (pre-stimulus). Then across all positions the maximum PSTH value was taken from 30-100ms time window where the maximum PSTH is expected to occur in response to the input stimuli. The corresponding time was also recorded.

Data Analysis: Latency

For each recording per neuron the latency corresponding to the maximum firing rate was determined. Latency refers to the time interval between the onset of the stimulus presentation and the response. The time corresponding to when the maximum stimulus occurred was used as a separate metric.

Data Analysis: PSTH vs Contrast

All neurons across all 156 recordings were first separated into two groups, monocular and binocular recordings based on the receptive fields of each recording. A receptive field less than or equal to 40 degrees in mouse visual space is classified as binocular, while any above 55 is monocular. Then each individual recording was further subdivided into the 7 different classes on contrast ranging from 0-100% that were present for both black and white input stimuli. The corresponding maximum PSTH was averaged across all neurons for a given contrast.

Results

Neurons that contribute to a response should have the same optimal receptive field as the LFP data. By hand, responses picked up by neurons residing in each layer were compared to the LFP data and marked as being a match versus mismatch based on the location of the optimal receptive field. In Figure 2a one can see an example of where the response was matched in all three layers. On the right is an example of a mismatched case, which can be most clearly seen by comparing layer 5/6. The suppression in the LFP data is around 50 degrees, while that for the spike data is closer to zero. Note that LFP data is flipped because of referencing, thus activation appears as a dark spot in LFP and a light spot in spike data. It is also worth noting that like in Figure 2b, some of the recordings did not have data corresponding to all three layers. In fact, many recordings had only data for layer 5/6 leading to a skewed sample size.

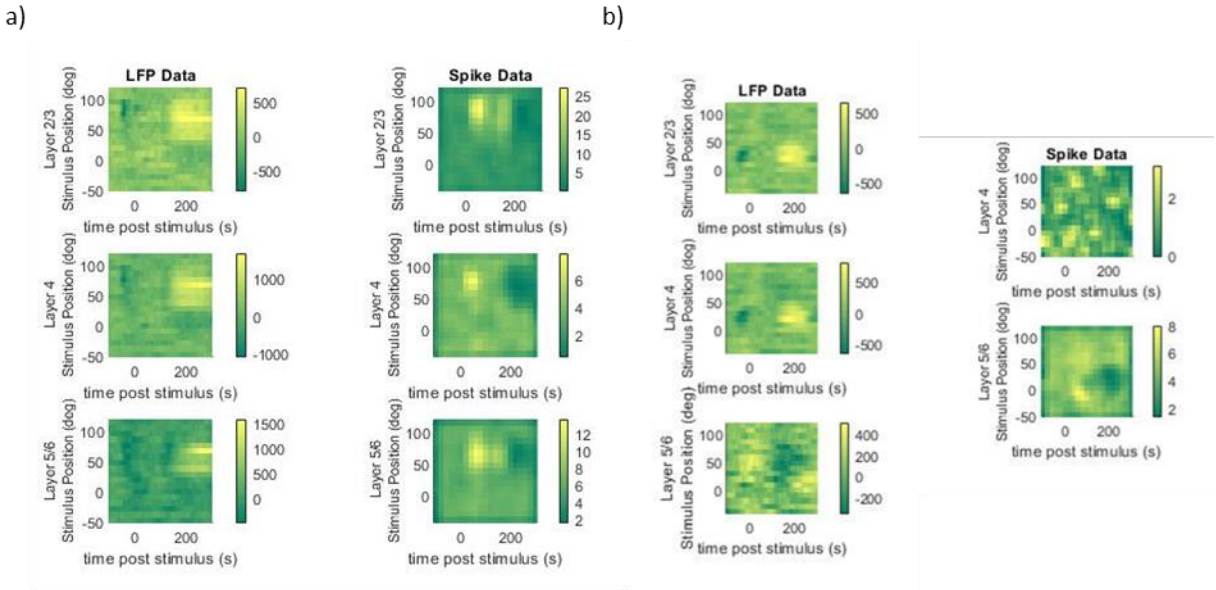

Figure 3 (a) Example of response that is matched across all layers. (b) Example of response that is not matched as seen clearly in layer 5/6. No data for neurons in layer 2/3 was collected.

Once all the spike data was compared to that of the LFP data the breakdown of data that matched and was used can be seen in Table 1. To further ensure that all data represents true peaks and not random noise only the neuron responses that were one standard deviation away from their individual response mean were taken.

The matched data can be divided into two classes based on the location of their optimal receptive field: monocular and binocular. These two groups relate to the monocular and binocular areas of V1 in which the probes were inserted. In each monocular and binocular group, you have FS and RS cells. The breakdown of this data can be seen in table 2. Aside from grouping the individual neurons, one can also divide the data into the 3 main layers of V1: layer 2/3, layer 4, and layer 5/6 as shown in table 3.

Layer	**Layer 2/3**	**Layer 4**	**Layer 5/6**
Matched	16	28	44
Mismatched	4	10	6

Table 1 Distribution of matched versus mismatched recordings

Cell Type	Monocular	Binocular
FS	953	1928
RS	1497	895

Table 2 Total number of recorded neuronal responses per trial per neuron type

Layer	Monocular	Binocular
L2/3	151	130
L4	656	534
L5/6	1643	2159

Table 3 Total number of recorded neuronal responses per trial per layer

Figure 4 and 5 below show the overall trend for Monocular and Binocular recordings when splitting both across cell type and layers. The black line represents the data corresponding to black bars, while the grey line is the white bars. The error bars correspond to the standard deviation of that data used for each point. Furthermore, for each data point Wilcoxon rank sum test was run. This is a nonparametric test for two populations with independent samples. It tests the null hypothesis that the data for black and white stimuli at a given contrast are from continuous distributions with equal medians. All green asterisk denotes the rejection of the null hypothesis with a 5% significance level. The noise seen in layer 2/3 across all figures can be attributed the small sample size. This is in part due to the fact that there are generally less neurons in layer 2/3.

When looking at the latency plots in Figure 4 the RS latency for black contrast is on average 0.004s faster than that of FS neurons. This is because RS neurons are putatively excitatory neurons while FS are putatively inhibitory. As a result, the RS neurons are the first to fire in response to a stimulus and are then suppressed by the FS neurons.

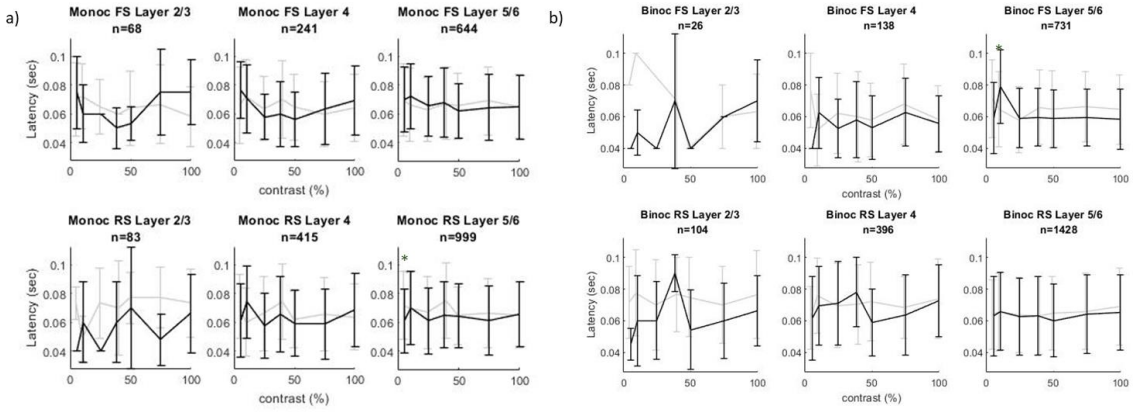

Figure 4 Latency versus contrast in monocular (a) and binocular (b) recordings, divided by cell type and across layers. Error bars represent 1 SD.

Looking at the PSTH plots in Figure 5 the RS firing is lower than that of FS neurons. This is due to the refractory period after the spike, which is very short in FS neurons, meaning they can fire another spike soon after the preceding one (Hu et. al., 2014). The magnitude of the response increases with increased contrast. These trends can most explicitly be seen in the data for layer 5/6 due to the large sample size.

In Figure 5b there is an observable black dominance in the binocular recordings in FS cells, specifically in layer 4 at 75% contrast, with $\mu_w = 7.373$ and $\mu_B = 12.616$. However, this difference is not statistically significant, p-value = 0.430 (Table 7). In monocular recordings on the left there is an observable small but uniform and consistent white dominance in the RS cells, but only statistically significant in layer 2/3 at 10% contrast with p-value of 0.042 (see appendix).

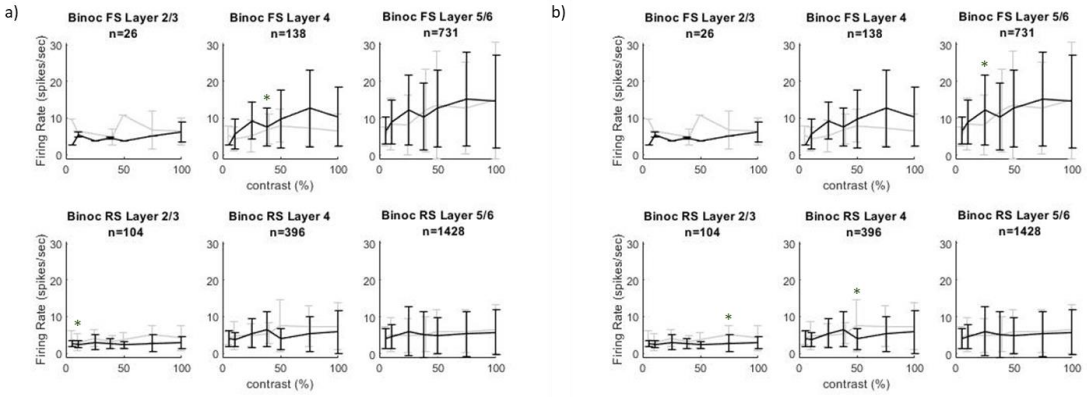

Figure 5 PSTH versus contrast in monocular(a) and binocular (b) recordings, divided by cell type and across layers. Error bars represent 1 SD.

Conclusion

The goal of this study was to characterize how excitatory and inhibitory neurons in the mouse V1 respond to dark and light visual stimuli, in both time and space. The trends in firing across time after stimulus presentation (Fig 5) do not show a statistically significant black dominance for FS cells in binocular recordings. When looking at the corresponding latencies in figure 4 one can see that blacks at higher contrasts (50-100%) in binocular FS recordings are processed on average 0.004s faster in layer 4 and 0.006s in layer 5/6 (see appendix). But the difference is not statistically significant. White dominance is also not statistically significant for RS cells in monocular recordings the only statistically significant point is in layer 2/3 at 10% contrast with p-value of 0.042 (see appendix). In figure 5 however, one can observed the white response as being uniform and consistent.

This study fails to confirm that the underlying mechanisms that are known to make up visual perception in higher primates, hold true in awake mice. This could be accredited to one of two things: the data set and the analysis. As mentioned, there are generally fewer neurons in layer 2/3 than in layer 5/6. This class imbalance can skew results as it becomes harder to generalize trends in smaller datasets which are prone to be affected by outliers. Prior to analyzing neuronal responses to input stimuli, the baseline activity of each neuron was calculated and removed as outline in the methods. Then to further ensure that all data represents true peaks and not random noise only the neuron responses that were one standard deviation away from their individual response mean were used for the analysis. This regularization of the data was heavily reliant on single neuronal responses at a given time point. It is possible that there are better methods of baseline subtraction and regularization of the data. One possibility would be to use the signal to noise ratio (SNR) rather than standard deviations as an indicator (Yeh et. al., 2009). It also possible that SNR can be used as a feature when looking to quantifying a cells response, rather than using the maximum firing rate.

As proven in literature neurons in V1 are sensitive to contrast where ON pathways prefer preference luminance increments while OFF pathways preference luminance decrements. However, these results do not indicate any statistically significant differences between these two pathways. In the future further analysis can be done using features which may reveal underlying trends that coincide with those in literature.

References

Buchner, A., & Baumgartner, N. (2007). Text – background polarity affects performance irrespective of ambient illumination and colour contrast. *Ergonomics*, *50*(7), 1036–1063. doi: 10.1080/00140130701306413

Buzsáki, G. (2004). Large-scale recording of neuronal ensembles. *Nature Neuroscience*, *7*(5), 446–451. doi: 10.1038/nn1233

Douglas RJ, Martin KAC (1998) Neocortex. In: The Synaptic Organization of the Brain, 4th Edition (shepherd GM, ed), pp. 459-510. New York: Oxford University Press.

Hu, H., Gan, J., & Jonas, P. (2014). Fast-spiking, parvalbumin + GABAergic interneurons: From cellular design to microcircuit function. *Science, 345*(6196), 1255263-1255263. Doi: 10.1126/science.1255263

Huberman, A. D., & Niell, C. M. (2011). What can mice tell us about how vision works? *Trends in Neurosciences*, *34*(9), 464–473. doi: 10.1016/j.tins.2011.07.002

Hubel, D. H., & Wiesel, T. N. (1959). Receptive fields of single neurones in the cats striate cortex. *The Journal of Physiology*, *148*(3), 574–591. doi: 10.1113/jphysiol.1959.sp006308

Jansen, M., Jin, J., Li, X., Lashgari, R., Kremkow, J., Bereshpolova, Y., … Alonso, J.-M. (2018). Cortical Balance Between ON and OFF Visual Responses Is Modulated by the Spatial Properties of the Visual Stimulus. *Cerebral Cortex*, *29*(1), 336–355. doi: 10.1093/cercor/bhy221

Kandel, E. R., Schwartz, J. H., Jessell, T. M., Siegelbaum, S. A., & Hudspeth, A. J. (2005). *Principles of neuroscience*. Appleton & Lange.

Kuffler, S. W. (1953). Discharge Patterns And Functional Organization Of Mammalian Retina. *Journal of Neurophysiology*, *16*(1), 37–68. doi: 10.1152/jn.1953.16.1.37

Komban, S. J., Alonso, J.-M., & Zaidi, Q. (2011). Darks Are Processed Faster Than Lights. *Journal of Neuroscience*, *31*(23), 8654–8658. doi: 10.1523/jneurosci.0504-11.2011

Niell, C. M. (2015). Cell Types, Circuits, and Receptive Fields in the Mouse Visual Cortex. *Annual Review of Neuroscience*, *38*(1), 413–431. doi: 10.1146/annurev-neuro-071714-033807

Pandarinath, C., Victor, J. D., & Nirenberg, S. (2010). Symmetry Breakdown in the ON and OFF Pathways of the Retina at Night: Functional Implications. *Journal of Neuroscience*, *30*(30), 10006–10014. doi: 10.1523/jneurosci.5616-09.2010

Piepenbrock, C., Mayr, S., Mund, I., & Buchner, A. (2013). Positive display polarity is advantageous for both younger and older adults. *Ergonomics*, *56*(7), 1116–1124. doi: 10.1080/00140139.2013.790485

Ryu, S. B., Werginz, P., & Fried, S. I. (2019). Response of Mouse Visual Cortical Neurons to Electric Stimulation of the Retina. *Frontiers in Neuroscience*, *13*. doi: 10.3389/fnins.2019.00324

Speed, A., Rosario, J. D., Burgess, C. P., & Haider, B. (2019). Cortical State Fluctuations across Layers of V1 during Visual Spatial Perception. *Cell Reports*, *26*(11). doi: 10.1016/j.celrep.2019.02.045

Wiebel, C. B., Singh, M., & Maertens, M. (2016). Testing the role of Michelson contrast for the perception of surface lightness. *Journal of Vision*, *16*(11), 17. doi: 10.1167/16.11.17

Woolsey, T. A., & Loos, H. V. D. (1970). The structural organization of layer IV in the somatosensory region (S I) of mouse cerebral cortex. *Brain Research*, *17*(2), 205–242. doi: 10.1016/0006-8993(70)90079-x

Xing, D., Yeh, C.-I., & Shapley, R. M. (2010). Generation of Black-Dominant Responses in V1 Cortex. *Journal of Neuroscience*, *30*(40), 13504–13512. doi: 10.1523/jneurosci.2473-10.2010

Yeh, C.-I., Xing, D., & Shapley, R. M. (2009). "Black" Responses Dominate Macaque Primary Visual Cortex V1. *Journal of Neuroscience*, *29*(38), 11753–11760. doi: 10.1523/jneurosci.1991-09.2009

Appendix

	2/3	4	5/6
FS	μ_w [0.07, 0.072, 0.065, 0.060, 0.064,0.067,0.058] μ_B [0.075,0.060,0.060,0.050,0.053,0.075,0.075] p-value [0.971,0.571,0.800,1,0.893,0.924,0.075]	μ_w [0.066,0.072,0.064,0.070,0.065,0.060,0.064] μ_B [0.076,0.071,0.058,0.060,0.056,0.064,0.069] p-value [0.345,0.851,0.573,0.389,0.297,0.780,0.399]	μ_w [0.070, 0.066, 0.063, 0.067, 0.065, 0.069, 0.065] μ_B [0.070, 0.072, 0.066, 0.068, 0.062, 0.064, 0.065] p-value [0.952, 0.280, 0.566, 0.904, 0.532, 0.348, 0.874]
RS	μ_w [0.073, 0.049, 0.073, 0.070,0.077,0.077,0.073] μ_B [0.040,0.060,0.040,0.060,0.070,0.048,0.066] p-value [0.200,0.558,0.571,0.697,0.944,0.066,0.546]	μ_w [0.071,0.060,0.066,0.075,0.062,0.066,0.064] μ_B [0.061,0.074,0.057,0.066,0.059,0.059,0.068] p-value [0.174,0.058,0.236,0.331,0.449,0.271,0.301]	μ_w [0.072,0.070,0.067,0.075,0.065,0.066,0.065] μ_B [0.061,0.070,0.061,0.065,0.064,0.061,0.066] p-value [0.010,0.962,0.220,0.108,0.807,0.200,0.858]

Table 1 Monoc latency mean (s) and p-value for white contrast and black contrast, divided by cell type and across layers. Corresponding to Figure 4a.

	2/3	4	5/6
FS	μ_w [0.080,0.100,0.070,0.040,0.060,0.063] μ_B [0.040,0.050,0.040,0.070,0.040,0.060,0.070] p-value [1,0.667,1,1,1,0.857]	μ_w [0.076,0.051,0.062,0.060,0.058,0.068,0.058] μ_B [0.040,0.063,0.053,0.058,0.053,0.063,0.056] p-value [0.571,0.324,0.477,0.933,0.796,0.805,0.788]	μ_w [0.071,0.065,0.0581,0.066,0.065,0.066,0.065] μ_B [0.059,0.079,0.059,0.060,0.059,0.059,0.059] p-value [0.069,0.009,0.639,0.206,0.355,0.164,0.052]
RS	μ_w [0.071,0.078,0.070,0.077,0.075,0.070,0.076] μ_B [0.045,0.060,0.060,0.090,0.054,0.060,0.066] p-value [0.103,0.298,0.654,0.581,0.358,0.592,0.238]	μ_w [0.062,0.076,0.070,0.070,0.072,0.068,0.073] μ_B [0.062,0.070,0.071,0.078,0.059,0.063,0.072] p-value [0.546,0.355,0.844,0.326,0.0788,0.480,0.685]	μ_w [0.064,0.066,0.064,0.063,0.065,0.066,0.069] μ_B [0.063,0.066,0.063,0.063,0.060,0.064,0.065] p-value [0.584,0.966,0.719,0.830,0.154,0.595,0.132]

Table 2 Binoc latency mean (s) and p-value for white contrast and black contrast, divided by cell type and across layers. Corresponding to Figure 4b.

	2/3	4	5/6
FS	μ_w [10.884,11.715,15.848,1.667,12.078,16.415,15.340] μ_B [4.708,13.059,35.196,4.549,24.412,19.196,13.287] p-value [0.486,0.897,0.267,0.667,0.571,0.914,0.805]	μ_w [9.224,7.409,9.857,10.809,9.896,12.740,12.303] μ_B [5.404,9.823,16.496,8.908,11.297,10.795,10.526] p-value [0.205,0.148,0.044,0.410,0.940,0.597,0.919]	μ_w [7.572,6.987,10.457,10.980,11.029,12.792,13.105] μ_B [6.165,7.707,12.619,14.507,12.678,12.6823,13.341] p-value [0.504,0.359,0.138,0.377,0.447,0.763,0.614]
RS	μ_w [2.123,1.516,4.085,5.709,8.064,9.734,7.978] μ_B [2.500,2.514,2.353,2.349,4.059,5.816,4.584] p-value [0.800,0.042,0.571,0.537,0.667,0.432,0.140]	μ_w [3.903,3.749,5.851,6.437,7.663,7.993,7.878] μ_B [3.691,4.948,5.425,3.962,6.540,6.176,7.750] p-value [0.903,0.132,0.357,0.097,0.791,0.135,0.919]	μ_w [4.723,5.831,8.126,7.036,9.845,10.306,9.579] μ_B [3.788,6.035,7.685,6.809,9.047,8.019,9.529] p-value [0.230,0.498,0.239,0.191,0.434,0.084,0.976]

Table 3 Monoc firing rate mean (spikes/sec) and p-value for white contrast and black contrast, divided by cell type and across layers. Corresponding to Figure 5a.

	2/3	4	5/6
FS	μ_w [9.630,6.481,4.775,10.784,6.699,6.324] μ_B [2.685,5.370,3.725,4.549,3.706,5.157,6.180] p-value [1,0.667,1,1,1,0.914]	μ_w [5.284,4.288,5.176,6.947,7.889,7.373,6.510] μ_B [2.685,5.588,9.248,7.475,9.760,12.616,10.317] p-value [0.571,0.638,0.167,0.940,0.949,0.430,0.174]	μ_w [4.962,8.372,8.212,12.076,13.555,12.774,14.814] μ_B [6.630,8.957,12.238,10.396,12.587,15.242,14.588] p-value [0.115,0.479,0.013,0.468,0.860,0.357,0.718]
RS	μ_w [4.0264,3.009,4.069,3.134,3.662,5.105,4.210] μ_B [2.546,2.400,2.922,2.539,2.319,2.654,2.815] p-value [0.315,0.845,0.222,0.476,0.230,0.028,0.368]	μ_w [4.105,4.697,4.937,5.475,7.581,7.377,7.386] μ_B [3.998,3.690,5.423,6.473,3.888,5.257,5.807] p-value [0.663,0.500,0.948,0.904,0.047,0.134,0.097]	μ_w [4.358,5.204,4.877,5.282,5.877,6.058,6.564] μ_B [4.058,4.610,6.071,5.23,4.952,5.361,5.766] p-value [0.449,0.692,0.443,0.241,0.391,0.198,0.160]

Table 4 Binoc firing rate mean (spikes/sec) and p-value for white contrast and black contrast, divided by cell type and across layers. Corresponding to Figure 5b.